PASJ: Publ. Astron. Soc. Japan **52**, ??–?? **(2008)**

arXiv:astro-ph/0002344v1 17 Feb 2000

Color–Magnitude Sequence in the Clusters at $z \sim 1.2$ near the Radio Galaxy 3C 324

Masaru Kajisawa, Toru Yamada, Ichi Tanaka
Astronomical Institute, Tohoku University, Aoba-ku, Sendai, Miyagi 980-8578
E-mail(MK): kajisawa@astr.tohoku.ac.jp

Toshinori Maihara, Fumihide Iwamuro, Hiroshi Terada, Miwa Goto,
Kentaro Motohara, Hirohisa Tanabe, Tomoyuki Taguchi, Ryuji Hata
Department of Physics, Faculty of Science, Kyoto University, Sakyo-ku, Kyoto 606-8502

Masanori Iye, Masatoshi Imanishi, Yoshihiro Chikada, Michitoshi Yoshida
National Astronomical Observatory, 2-21-1 Osawa, Mitaka, Tokyo 181-8588

Chris Simpson, Toshiyuki Sasaki, George Kosugi, Tomonori Usuda
and
Kazuhiro Sekiguchi
Subaru Telescope, National Astronomical Observatory of Japan,
650 North Aohoku Place, Hilo, HI 96720, U.S.A.

(Received 1999 November 26; accepted 1999 December 22)

Abstract

We have investigated the optical and near-infrared colors of K'-selected galaxies in clusters at $z \sim 1.2$ near to the radio galaxy 3C 324 using images obtained with the Subaru telescope and archival HST data. The distribution of colors of the galaxies in the cluster region is found to be fairly broad, and it may imply significant scatter in their star-formation histories, although the effect of contamination of field galaxies is uncertain. The red sequence of galaxies whose $R - K$ colors are consistent with passive evolution models for old galaxies is found to be truncated at $K' \sim 20$ mag, and there are few fainter galaxies with similar red colors in the cluster region. We find that the bulge-dominated galaxies selected by quantitative morphological classification form a broad sequence in the color–magnitude diagram, whose slope is much steeper than that expected from metallicity variations within a passively evolving coeval galaxy population. We argue that the observed color–magnitude sequence can be explained by metallicity and age variations, and the fainter galaxies with $K' > 20$ mag may be 1–2 Gyr younger than the brighter galaxies. Some spatial segregation of the color and K'-band luminosity is seen in the sky distribution; the redder and the brighter objects tend to be located near 3C 324.

Key words: galaxies: clusters of — galaxies: evolution — galaxies: formation

1. Introduction

By tracing the average properties of galaxies in rich clusters and their progenitors from low to high redshift, we can study how galaxies in similar environments evolve with cosmic time, and obtain insights into the phenomenon of galaxy formation. In nearby and intermediate-redshift clusters, the majority of bright galaxies are known to form a tight and conspicuous red sequence in the color–magnitude diagram (e.g., Visvanathan, Sandage 1977; Bower et al. 1992). This color–magnitude (hereafter C–M) relation seen in nearby clusters extends over a range of at least 4-magnitudes (Garilli et al. 1996) and possibly 5–6 mag (e.g., De Propris et al. 1998) from the brightest cluster galaxies; the slope of the relation does not vary from cluster to cluster. Bower et al. (1992) showed that the small dispersion of the C–M relation for early-type galaxies in the Coma and Virgo clusters places a strong constraint on their age or coevality by assuming a simple star-formation history; they found that the early-type galaxies in these clusters are older than $\sim$ 10 Gyr, if an age spread of $\sim$ 1 Gyr is assumed (see Bower et al. 1998 for more general discussion). Aragón-Salamanca et al. (1993) then found a systematic evolution in the colors of the reddest cluster members which they interpreted as being passive evolution of old galaxies formed at $z \gtrsim 2$. Ellis et al. (1997) and Stanford et al. (1998) investigated *morphologically selected* early-type galaxies in intermediate-redshift clusters, and found that the well-defined C–M sequence with small scatter holds there. Gladders et al. (1998) also found that the evolution of the slope of the C–M sequence is consistent with the predictions of passive evolution. These conclusions from studies of the C–M relation are complemented by those from Fundamental Plane analysis (e.g., van Dokkum et al. 1996, 1998). The C–M relation is more favorably interpreted as being a metallicity sequence, rather than an age sequence, since otherwise the slope should be much steeper than observed even at an intermediate redshift (Kodama, Arimoto 1997), although some age difference between bright and faint galaxies has been pointed out by some authors based on the observed differences in the absorption-line strength (e.g., Terlevich et al. 1999).

On the other hand, there are many observational indications that the star-formation activity in more distant clusters is higher than that in local clusters. It is known that the fraction of blue galaxies in clusters increases rapidly with the redshift at intermediate-redshift (Butcher, Oemler 1978, 1984; Rakos, Schombert 1995). Rakos and Schombert showed that the fraction of blue galaxies becomes $\sim 80\%$ at $z = 0.9$. Through spectroscopic studies of intermediate-redshift clusters, it is also known that a significant fraction of galaxies have emission-lines and/or post-starburst signatures (e.g., Dressler, Gunn 1992; Postman et al. 1998; Dressler et al. 1999; Poggianti et al. 1999). Postman et al. (1998) investigated two clusters at $z \sim 0.9$ spectroscopically, and found that about half of the galaxies show high levels of star formation activity. It is expected from these results that a more active evolution of galaxies may be observed in clusters at higher redshift.

Recently, a number of clusters and cluster candidates at $z \gtrsim 1$ have been discovered (Dickinson 1995; Yamada et al. 1997; Stanford et al. 1997; Hall, Green 1998; Benítez et al. 1999; Tanaka et al. 1999; Rosati et al. 1999). By observing high-redshift clusters, any differences in the star-formation history can be seen more clearly. Tanaka et al. (1999) investigated the colors of galaxies in the cluster 1335.8+2820 at $z \sim 1.1$, and showed that the optical and near-infrared color distributions of the galaxies in this cluster are wide, which may be attributed to variations in the star-formation activity. They found that the fraction of galaxies which show some UV excess over the expected colors for passive evolution is more than 75% in this cluster. Stanford et al. (1997) investigated the NIR-selected cluster CIG J0848+4453 at $z = 1.27$, and also showed that those galaxies whose RJK colors are consistent with passively evolving elliptical models have relatively blue $B - K$ colors, which indicates that some star-formation activity is occurring in the old galaxies in the cluster core. It is therefore interesting to expand the detailed color analysis to other clusters at $z \gtrsim 1$, and to see whether these results apply generally to high-redshift clusters.

In this paper, we consider the optical and near-infrared (NIR) colors of K'-selected galaxies in those clusters at $z \sim 1.2$ near to the radio galaxy 3C 324 (Dickinson 1997a,b; Kajisawa, Yamada 1999; Kajisawa et al. 2000, hereafter as Paper I) using images obtained with the Subaru telescope and archival data from the Hubble Space Telescope (HST).

An excess of galaxy surface density in this region was recognized by Kristian et al. (1974) and by Spinrad and Djorgovski (1984), and firmly identified by Dickinson (1995). In Dickinson's (1997b) spectroscopic study, the surface-density excess was revealed to be due to the superposition of two clusters or rich groups at $z = 1.15$ and $z = 1.21$. Extended X-ray emission with a luminosity comparable to that of the Coma cluster has been detected in the direction of 3C 324 (Dickinson 1997a), which suggests that at least one of the two systems is a fairly collapsed massive system. Smail and Dickinson (1995) detected a weak shear pattern in the field that may be produced by a cluster. In the following discussion, we do not distinguish the two systems at $z \sim 1.2$, since a detailed redshift distribution of the galaxies or the relative population of them is still not available. We thus discuss the average properties of the two clusters. Since their redshifts are close, it has little effect on our discussion about the luminosity and color distributions.

Using a K'-selected sample provides such advantages as (i) the selection bias at large redshift is small, and thus a direct comparison with lower-redshift clusters is possible (Aragón-Salamanca et al. 1993) and (ii) the sample selection is less affected by the star-formation activity. Furthermore, the rest-frame mid-UV color provided by the HST data enables us to detect even a small amount of recent star-formation (e.g., Ellis et al. 1997; Smail et al. 1998). We describe the observations and data reduction briefly in section 2. In section 3, we present the color-magnitude and two-color diagrams. Our conclusions and discussions are given in the last section.

In a previous Paper I, we studied the K-band luminosity distribution of the galaxies in these clusters near to 3C 324 using the same K'-band data, which is closely related to the results presented here. In summary, Paper I showed that the shape of the bright end ($K \lesssim 20$) of the luminosity function is similar to those of lower-redshift clusters; also the measured value of the characteristic magnitude, K^*, follows the evolutionary trend of intermediate-redshift clusters, which is consistent with passive evolution models with $z_{\rm form} \gtrsim 2$. At the faint end, however, the excess galaxy surface density within 40" of 3C 324 decreases abruptly at $K \sim 20$, which may indicate a strong luminosity segregation with distance from 3C 324 or a real deficit in the faint galaxy population in the clusters. Kajisawa and Yamada (1999) also presented results from a study of the colors and morphologies of an *optically selected* sample of cluster galaxies using the same HST data.

2. Observations and Data Reduction

2.1. K'-Band Image

K'-band imaging of the 3C 324 field was carried out with the Cooled Infrared Spectrograph and Camera for OHS (CISCO, Motohara et al. 1998) mounted on the Subaru Telescope on 1999 April 1 and 2 (UT), during the telescope commissioning period. The detector is a 1024 × 1024 HAWAII HgCdTe array with a pixel scale of 0."116, which provides a field of view of ∼ 2' × 2'. The presently images studied are common to those analyzed in Paper I. See Paper I for details concerning the data reduction. The seeing size of the resultant frame is 0."8 arcsec as measured from the FWHM of the stellar images.

A flux calibration was performed by observing one the UKIRT Faint Standard FS 27 immediately after the 3C 324 field at a similar zenith distance. We used the empirical relation $K' - K = 0.2(H - K)$ (Wainscoat, Cowie 1992) in order to derive the K' mag of FS 27 from its H and K mag.

Source detection was performed with the SExtractor image analysis package (Bertin, Arnouts 1996). We used a detection threshold of $\mu_{K'} = 22.4$ mag arcsec^{-2} over 20 connected pixels. We removed from the final catalog those bright objects with $K' < 18$, which appeared unresolved. Although we did not make any star/galaxy separation at $K' > 18$, the contamination by stars in the catalogue is small at $K' > 18$ (at most $\sim 5 - 10\%$; De Propris et al. 1999). In total, 146 sources were cataloged. We used a 3" diameter aperture to measure the K' mag of the objects and a 1."6 one to derive the colors.

2.2. Optical Images

To investigate the colors of the K'-selected galaxies, we analyzed the archival HST/WFPC2 F702W and F450W images of the 3C 324 field (PI: M.Dickinson; PIDs 5465 and 6553, respectively). The total exposure times were 64800 sec for the F702W image and 17300 sec for the F450W image.

After combining the separate exposures with cosmic-ray rejection, we aligned the F702W and the F450W images to the K' image using point sources common to the frames. The optical images were then convolved with a Gaussian kernel to match the FWHM of the stellar images in the K' frame. Photometry of each K'-selected object was performed using apertures with identical positions and size (1."6 diameter) regarding the K' image in each optical frame. We used the STMAG system for these optical magnitudes, and hereafter refer them as $R_{\rm F702W}$ and $B_{\rm F450W}$ (STMAG is defined as $m_{\rm ST} = -21.10 - 2.5\log f_\lambda$ where f_λ is expressed in erg cm^{-2} s^{-1} Å^{-1}; HST Data Handbook Vol.1). Due to the limitation of the WFPC2 field of view (figure 10), the number of K'-selected galaxies for which $R_{\rm F702W}$ and $B_{\rm F450W}$ mag were measured is 139.

3. Results

3.1. Color–Magnitude Diagram

Figure 1 shows the C–M diagram (K' vs $R_{\rm F702W} - K'$) of the detected galaxies. We have divided the observed frame into the 'cluster' region (within 40" of 3C 324) and the 'outer' region (the remainder of the frame); note that a clear excess of galaxies with $K \lesssim 20$ mag in the 'cluster' region has been recognized at $\sim 10\sigma$ significance (Dickinson 1995; Paper I). The areas of the 'cluster' and the 'outer' regions are 1.193 arcmin^2 and 1.877 arcmin^2, respectively, and the galaxies in each region are plotted with different symbols in the figure. The error bars are based on the 1σ background fluctuation within a 1."6 aperture. The dotted line represents the ∼ 70% completeness level of $K' = 21.5$ (Paper I). The dashed line shows $R_{\rm F702W} = 28$ mag, which corresponds to the $\sim 3\sigma$ detection limit in this band. Most of the K'-selected galaxies, except for a few extremely red objects, have $R_{\rm F702W}$ magnitudes brighter than this limit.

In figure 1, the red envelope of the galaxies with $R_{F702W} - K' \sim 6$ can be seen, and those objects with $K' \lesssim 21$ mag and $R_{\rm F702W} - K' > 4.5$ are dominated by the galaxies in the 'cluster' region, despite the area of the outer region being 1.6-times larger than that of the cluster region. In the magnitude range $17 < K' < 21$, there are 6±2, 8±1, and 5±3 cluster galaxies with $R_{\rm F702W} - K' > 5.5$, $4.5 < R_{\rm F702W} - K' < 5.5$, and $R_{\rm F702W} - K' < 4.5$, respectively, after applying a field correction using the 'outer' region. The quoted uncertainties are based on Poisson statistics. Thus, about one-third of the cluster galaxies with $K' < 21$ mag have $R_{\rm F702W} - K' > 5.5$ and their stellar populations are expected to be fairly old ($\gtrsim$ 2 Gyr); a more detailed comparison with the galaxy evolutionary models is presented below.

We confirm the existence of the 'red finger', a sequence of galaxies with $R_{\rm F702W} - K' \sim 6$ and $K' \sim$ 18–19 mag, which was identified by Dickinson (1995). The observed colors of these galaxies are consistent with Dickinson's result if we consider $R_{\rm F702W} - R$ and $K' - K$ color differences. Kodama et al. (1998) derived the slope and zero point of this 'red finger' using the data of Dickinson (1995), and showed that the sequence is consistent with a metallicity sequence at $z \sim 1.2$ for passively evolving galaxies. This red sequence of galaxies in the cluster region, however, seems to be truncated at $K' \sim 20$. Although there are a few red objects in the outer region, there is no such object in the cluster region fainter than this magnitude. This is *not* due to incompleteness; at $K' \sim 21$ the catalog is still $\sim 90\%$ complete (Paper I). To emphasize this point, figure 2 shows the number counts of the 'red sequence' galaxies with $5.7 < R_{\mathrm{F702W}} - K' < 6.3$, which corresponds to the color range adopted in Kodama et al. (1998), together with the detection completeness in the K'-band evaluated in Paper I.

Another important aspect of the C–M diagram in figure 1 is that the color distribution of galaxies in the cluster region is fairly wide: in addition to the 'red sequence' galaxies, there are many galaxies with bluer $R_{\mathrm{F702W}} - K'$ colors in the cluster region. There seems to exist an even more significant surface density excess within the 'cluster' region in the range $4.5 < R_{\mathrm{F702W}} - K' < 5.5$ ($\sim 8 \pm 1$ cluster galaxies) compared with those in the $R_{\mathrm{F702W}} - K' > 5.5$ range ($\sim 6 \pm 2$ cluster galaxies). At $R_{\mathrm{F702W}} - K' < 4.5$, a marginal excess of cluster-region galaxies can also be seen (5 ± 3 cluster galaxies). The galaxies with bluer $R_{\mathrm{F702W}} - K'$ colors tend to be fainter at K'. The median magnitude of the galaxies with $4.5 < R_{\mathrm{F702W}} - K' < 5.5$ is $K' \sim 20$, while that of the redder ones is $K' \sim 19$.

3.2. *Two Color Diagram*

The wide spread in the optical-NIR colors may be due to age differences and/or ongoing star formation as well as to contamination by foreground/background galaxies. To investigate the causes of the large scatter in the C–M diagram, we show a $B_{\mathrm{F450W}} - R_{\mathrm{F702W}}$ vs $R_{\mathrm{F702W}} - K'$ two-color diagram for the galaxies with $K' < 22$ in figures 3 and 4. The shaded and open symbols in figure 3 represent the galaxies in the 'cluster' and the 'outer' regions, respectively. The arrows show that the objects are fainter than the 3 σ upper limit of $B_{\mathrm{F450W}} = 26$.

In figure 4, we add the model colors of galaxies with various star-formation histories observed at $z = 1.2$, using the GISSEL96 code (Bruzual, Charlot 1993), and adopting the Salpeter initial mass function. We examined the star formation models with a 1 Gyr single burst, exponentially decaying star-formation rates with timescales $\tau = 0.5$ and 1 Gyr, and a constant star formation rate (SFR). We also investigated a 1 Gyr single burst model with a metallicity of 0.2-times the solar value, and confirmed that the differences between it and the solar-metallicity model are seen along the 'age direction', as expected from the "age–metallicity degeneracy". The colors of the models of old-population plus ongoing starburst are also plotted; to produce these we have added the constant SFR models with an age of 0.1 Gyr and mass fractions from 0.02% to 0.5% to the old single-burst models. It can be seen that these models may be mimicked by the exponentially decaying models. Note that these models have much redder colors than those for spiral galaxies, which are characterized by $\tau >$ 2 Gyr (Bruzual, Charlot 1993).

It is found from figure 4 that the colors of the galaxies in the red sequence, $R_{\mathrm{F702W}} - K' > 5.5$, are consistent with those of the models whose age is 3–4 Gyr, irrespective of the existence of a small amount of ongoing star formation.

On the other hand, many of the galaxies with $4.5 < R_{\mathrm{F702W}} - K' < 5.5$ are more consistent with the models with a younger age, 1–3 Gyr, and are insensitive to the amount of star-formation activity, if we assume they are at the same redshift and neglect possible reddening by dust. The bluer $R_{\mathrm{F702W}} - K'$ colors must be due, at least in part, to a younger age, since the $B_{\mathrm{F450W}} - R_{\mathrm{F702W}}$ color would be $\sim$ 0.5–1 mag bluer than observed if the bluer $R_{\mathrm{F702W}} - K'$ colors were purely due to star-formation activity. In fact, the bluer $R_{\mathrm{F702W}} - K'$ colors must be *predominantly* due to a youthfulness effect for objects with $B_{\mathrm{F450W}} - R_{\mathrm{F702W}} \gtrsim 0$, which are less affected by star formation. Note that the effect of metallicity on the age estimation is small in this range. Although there may be effects of dust extinction, the reddening arrow (Cardelli et al. 1989) in figure 4 is almost parallel to the lines of constant age. There are also some galaxies in the color range $B_{\mathrm{F450W}} - R_{\mathrm{F702W}} \lesssim 0$ and $R_{\mathrm{F702W}} - K' \sim 4$, which may be consistent with $\sim$ 1 Gyr-old galaxies at $z = 1.2$ or galaxies with strong star-formation, although the contamination by foreground/background galaxies is expected to be large in this color range. From these results, both the ages and star formation histories of the 3C 324 cluster galaxies appear to have significant scatter.

In figure 4, we have further divided the K'-selected galaxies into two samples with $K' < 20$ (circles) and $20 < K' < 22$ (squares). As inferred from figure 2, there are few 'red sequence' galaxies with $K' > 20$ mag. On the other hand, most galaxies with $R_{\mathrm{F702W}} - K' \sim 4.5$ whose colors are consistent with those at $z \sim 1.2$ have $K' > 20$. The population with $R_{\mathrm{F702W}} - K' \sim$ 4.5–5.5 is a mixture of the bright and faint samples. There may be a trend that galaxies with younger ages or stronger star-formation activity are fainter in the K'-band. Postman et al. (1998) investigated two clusters at $z \sim 0.9$, and showed the existence of a correlation between the 'color age' and luminosity (their figures 18 and 19). The 3C 324 clusters may have a similar property.

The arguments about the star-formation histories of the galaxies presented above are based on the assumption that many of these red galaxies are indeed at $z = 1.2$. In order to further understand the properties of the cluster galaxies, we filtered the sample to be less contaminated by the foreground galaxies. Most of the galaxies with $R_{\rm F702W} - K'$ bluer than the passive evolution models at $z = 1.2$ at a given $B_{\rm F450W} - R_{\rm F702W}$ color are considered to be in the foreground. We tentatively divided the two-color diagram into two color domains of '$z = 1.2$' and 'foreground' using as a boundary the 1 Gyr burst model with 0.2 solar metallicity. The galaxies in the '$z = 1.2$' color domain are expected to be dominated by the cluster members, although some of them may be dusty foreground galaxies or relatively young galaxies at a higher redshift. As a further check, we compared the number counts of galaxies in the 'foreground' color domain located in the 'cluster' region with the general field counts derived by averaging the number counts taken from the literature (see Paper I) in figure 5. They are fairly consistent down to $K \sim 21.5$, where our detection incompleteness becomes as large as $\sim 30\%$.

At $K \gtrsim 20$, even the total number counts of the 'cluster' region are slightly lower than the average field counts. At the same time, there are not as many galaxies in the 'cluster' region with $K > 20$ in the '$z = 1.2$' color domain, as expected for a luminosity function with a steep faint-end slope, $\alpha \lesssim -1$. For example, there are four galaxies in the'$z = 1.2$' color domain between $20.5 < K' < 21.5$, while the expected number is 9.1 for $\alpha = -0.9$ (Paper I). The apparent deficiency of the surface density excess in the 'cluster' region discussed in Paper I may thus be at least partly due to the intrinsically small number of cluster galaxies, although it is still highly uncertain how many of the four galaxies are in the background and how many cluster galaxies may have been missed by the color selection: complete spectroscopic surveys or more accurate photometric redshift measurements are needed to determine the precise number of cluster galaxies at faint magnitude levels.

3.3. *Properties of the Color-Selected Galaxies*

Using the criteria described above, we investigated the properties of the 'color-selected' cluster galaxy candidates. First, we applied a quantitative morphological classification to those galaxies in the '$z = 1.2$' color domain, using the WFPC2 $R_{\rm F702W}$ image. The classification was performed using the central concentration index, C, and the asymmetry index, A, to separate early-type (bulge dominated), late-type (disk dominated), and irregular galaxies (Abraham et al. 1996). Our procedure for measuring the C and A indices followed Abraham et al. (1996), except that we adopted the centering algorithm of Conselice et al. (1999). Early-type galaxies show a strong central concentration, while late-type galaxies have a lower concentration. Irregular galaxies have a high asymmetry.

We divided the galaxies in the '$z = 1.2$' color domain into several $R_{\rm F702W}$ magnitude bins. Since the C and A indices depend on object brightness, even if the intrinsic light profiles are identical, the boundaries between morphological types in the log C–log A plane should be determined separately for each magnitude bin. The boundaries are determined with the help of simulated galaxy images produced with the IRAF ARTDATA package. For this purpose, we constructed artificial galaxies with pure de Vaucouleurs (bulge) or pure exponential (disk) profiles with a similar range of half-light radii as the observed galaxies. The C and A indices of these artificial galaxies were measured in an identical manner to the real ones. As a result of this simulation, we divided the morphological classes as shown in figure 6. Although the artificial galaxies have no intrinsic irregularity, their apparent asymmetry arises from the addition of noise, we adopted the 90% completeness limit as the boundary of the irregular galaxies in each magnitude bin. We set the boundary between the bulge and disk-dominated galaxies so that the fractions of correctly classified galaxies in each sample would be equal. The resultant completeness of this bulge/disk classification is $\sim 90\%$ for the $R_{\rm F702W}$ = 24–25 mag bin and $\sim 70\%$ for the 27–28 mag bin. The resultant classification for the observed galaxies within the '$z = 1.2$' color domain is shown in figure 7.

In figure 8, we show the F702W-band montage of those galaxies having '$z = 1.2$' colors. The top three rows are for those galaxies classified as 'bulge-dominated', the middle three rows are the 'disk-dominated' galaxies, and the bottom three rows are the 'irregular' galaxies. Our morphological classification seems to work well. Each of the three rows for each morphological type represents a range of $R_{\rm F702W} - K'$ color. It can be seen that about half of the bulge-dominated galaxies have relatively blue colors ($R_{F702W} - K' < 5.5$). On the other hand, there are several red ($R_{\rm F702W} - K' > 5.5$) disk-dominated galaxies; this may imply that star-formation activity has ceased in these objects, or it may be an effect of dust reddening, although there may also be some contamination by 'bulge-dominated' or background galaxies. The relatively large number of 'irregular' galaxies may indicate that galaxy interactions occur frequently in the 3C 324 clusters.

Dickinson (1997b) presented a montage of the spectroscopically confirmed cluster members at $z = 1.15$ and $z = 1.21$ using the same $R_{\rm F702W}$-band image. Although he did not identify things such as the coordinates, we visually compared our reduced image with his figure 3 and confirmed that not only some red galaxies, but also some blue galaxies in figure 8 are really cluster members. Of the fifteen spectroscopically confirmed cluster members (excluding 3C 324 itself) in figure 3 of Dickinson (1997b), we identified seven red ($R - K > 5.5$) galaxies and three bluer galaxies within the '$z = 1.2$' color domain from their morphology and environment. We also found that three spectroscopically confirmed cluster galaxies lie in the foreground color domain near to the boundary ($B_{\mathrm{F450W}} - R_{\mathrm{F702W}} \sim -0.6$, $R_{\mathrm{F702W}} - K' \sim 3.8$). It may not be surprising that some blue-cluster galaxies were missed in our color selection, since the boundary of the color domain is for the ideal model galaxies and there may be an effect of dust reddening in the UV flux.

Figure 9 shows the C–M diagram for the galaxies in the '$z = 1.2$' color domain with their morphological classifications. A morphological classification was not assigned for a few faint galaxies whose surface brightness in the R_{F702W}-band was too low.

We compare the colors and magnitudes of the bulge-dominated galaxies with the metallicity-sequence model for early-type galaxies calibrated with the Coma cluster C–M relation (Kodama, Arimoto 1997) using the Kodama and Arimoto population synthesis model (solid line). The model galaxies are formed coevally at $z_{\mathrm{f}} = 4.5$ and then evolve passively. Clearly, the observed colors of the bulge-dominated galaxies are not compatible with the model prediction, and the fainter objects are ~ 1 mag bluer than the model prediction. In fact, the bulge-dominated galaxies in the 'cluster' region seem to form a rather broad sequence with a much steeper slope from $R_{\mathrm{F702W}} - K' \sim 6$ and $K' \sim 18$ to $R_{\mathrm{F702W}} - K' \sim 4.5$ and $K' \sim 21$.

In figure 10, we show the sky distribution of the galaxies in the '$z = 1.2$' color domain. The distribution of the galaxies seems to have an irregular structure and some spatial segregation between bright and faint sample can be seen; the redder and brighter galaxies tend to be located around 3C 324, while the bluer or fainter galaxies have a more diffuse distribution. While the surface densities of the color-selected galaxies with $K < 20$ are 12.6 arcmin^{-2} and 2.1 arcmin^{-2} in the cluster region and the outer region, respectively, the densities of the fainter galaxies are 7.5 arcmin^{-2} and 5.9 arcmin^{-2}. Similarly, while the surface densities for the red ($R_{\mathrm{F702W}} - K' > 5.5$) galaxies are 6.7 arcmin^{-2} and 2.1 arcmin^{-2}, those for the bluer galaxies are 12.6 arcmin^{-2} and 6.4 arcmin^{-2}. The color segregation therefore seems to be weaker than the luminosity segregation.

4. Discussion

We have presented the color distribution of the K'-band selected galaxies in the region of the clusters at $z = 1.2$ near to the radio galaxy 3C 324. While the 'red finger', a sequence of galaxies with $R_{\mathrm{F702W}} - K' \sim 6$ and $K' \sim$ 18–19 whose colors are consistent with ages $\gtrsim 3$ Gyr (or $z_{\mathrm{f}} > 4.5$; see Kodama et al. 1998) was recognized in the color-magnitude diagram, we also found that this sequence is truncated at $K' \sim 20$ mag; also, few galaxies in the 'cluster' region with fainter magnitudes have similar red colors. Garilli et al. (1996) presented optical C–M diagrams ($g - r$ vs r) for 67 low-redshift Abell and EMSS clusters, where most of these clusters show a red sequence extending over more than 4 magnitudes. De Propris et al. (1998) presented a C–M diagram ($B - R$ vs H) for the Coma cluster, where the C–M relation for early type galaxies ranges over more than 5 mag. Compared with these low-redshift clusters, the 'red sequence' of the 3C 324 clusters is clearly truncated.

We investigated the significance of this truncation, assuming that the red sequence population has a K-band luminosity distribution whose shape is identical to the cluster population as a whole. We assumed a faint-end slope of $\alpha = -0.9$, and adopted a characteristic magnitude of $K^* = 18.4$ (Paper I). The normalization was determined from the observed number of red sequence galaxies with $17 < K < 20$, and the expected number of red galaxies with $20 < K < 21$ was estimated, taking incompleteness into account. The estimated number of red galaxies with $5.7 < R_{\mathrm{F702W}} - K' < 6.3$ and $20 < K < 21$ is 3.63 in the cluster region and 4.85 for the entire region, while the observed numbers are 0 and 1, respectively.

We also investigated the $B_{\mathrm{F450W}} - R_{\mathrm{F702W}}$ vs $R_{\mathrm{F702W}} - K'$ two-color diagram and compared the observed colors with models of various star-formation histories, assuming that the galaxies are indeed at $z = 1.2$. We found that the large scatter in $R_{\mathrm{F702W}} - K'$ is due to variations in both the age and star-formation activity, and that the objects with bluer $R_{\mathrm{F702W}} - K'$ colors have younger ages than the 'red finger' objects, provided that they are not dominated by foreground/background galaxies.

For moderately red objects with $4.5 < R_{\mathrm{F702W}} - K' < 5.5$ and $B_{\mathrm{F450W}} - R_{\mathrm{F702W}} > 0$, the bluer $R_{\mathrm{F702W}} - K'$ color is found to be mainly due to younger ages. There is a trend that galaxies with fainter K' mag have bluer colors. Because the near-infrared K' magnitude can be an approximate measure of the total stellar mass for quiescent galaxies, it may imply that the relatively low-mass galaxies are, on average, younger than the massive galaxies in the 3C 324 clusters.

The 'bulge-dominated' galaxies within the cluster region seem to form a broad color-magnitude sequence whose slope is much steeper than predicted by coeval passive-evolution models. From the above discussion, this can be interpreted as an effect of the age sequence in addition to the metallicity sequence, provided that the galaxies really are cluster members. For a comparison, in figure 9, we also plot the 'metallicity plus age' sequence model, using the Kodama and Arimoto code. In this model, the zero point is the same as the pure metallicity-sequence model discussed in the previous section at $R_{\mathrm{F702W}} - K' = 6$ ($z_{\mathrm{f}} = 4.5$, ~ 3 Gyr old), and the fainter galaxies are 0.5 Gyr younger per 1 M_V-magnitude (at $z = 0.02$). The mean metallicity at each magnitude is adjusted so that the model sequence coincides with the Coma cluster C–M relation, when it is evolved passively to $z = 0.02$. It can be seen that this model well reproduces the sequence of the 'bulge-dominated' cluster-region galaxies. The age difference may thus be as much as ~ 2 Gyr between galaxies with $K' = 18$ and $K' = 21$.

Is this picture consistent with the well-defined C–M sequence observed in intermediate-redshift clusters? The C–M relation of morphologically selected early-type galaxies in clusters at $z = 0.2$–0.8 is known to extend over a range of at least 3–4 magnitudes with a scatter smaller than 0.1 mag (e.g., Ellis et al. 1997; Stanford et al. 1998). This is very different from the C–M sequence observed at $z = 1.2$. However, if the relatively large scatter and steep slope of the C–M relation for the bulge-dominated galaxies in the 3C 324 clusters are caused by an age difference and the evolution is passive after $z = 1.2$, the younger (bluer) galaxies would change their color and luminosity more rapidly than the old (red) galaxies, and may become as red as and even fainter within a relatively short time. The C–M relation would then become tighter and would extend over a larger magnitude range, with a shallower slope. Note that the effect of an additional small amount of star formation at $z = 1.2$ with a standard IMF is negligible at intermediate-z, if the star formation ceases immediately after $z = 1.2$, because the brightness of these component declines rapidly as massive stars die and the main sequence burns down.

For example, we compared the color and luminosity evolution of the 1 Gyr burst models with different ages, using the GISSEL96 code. One model is 3 Gyr old at $z = 1.2$ (formation redshift $z_{\rm f} \sim 5$, $H_0 = 50$ km s^{-1} Mpc^{-1}, $q_0 = 0.5$) and its optical–NIR color is $R_{\rm F702W} - K' \sim 6$, which roughly corresponds to the 'red sequence' population. The other is 1.5 Gyr old at $z = 1.2$ ($z_{\rm f} \sim 2$) and its $R_{\rm F702W} - K' \sim 5$, which represents the bluer galaxies. At $z \sim 0.7$, the difference in $R_{\rm F702W} - K'$ color between these two models is only $\Delta(R_{\rm F702W} - K') \sim 0.1$, and the difference in $B_{\rm F450W} - R_{\rm F702W}$ color, which is more sensitive to a small amount of star formation, becomes ~ 0.1 by $z \sim 0.5$. The fading of the younger model galaxy in the K' band is about 0.5 mag greater than that of the old model galaxy at $z \lesssim 0.9$; if we assume that the younger galaxy is about 1 magnitude fainter at $z = 1.2$, it becomes about 1.5 magnitude fainter at an intermediate redshift. From these results, the bluer 'bulge-dominated' population in the 3C 324 clusters is expected to form a fainter part of the tight C–M relation at intermediate-redshift, which may at least partially explain the observed apparent truncation of the red sequence at $z = 1.2$.

In Paper I, we showed that the excess of the surface density in the cluster region drops abruptly at $K \sim 20$ mag. One possible interpretation is that there may be an intrinsic deficit of faint galaxies in the clusters. Despite the existence of color selected galaxies with $K > 20$ mag in the cluster region, this possibility cannot be completely ruled out, since the number of these objects may not be large enough (subsection 3.2). There is, however, another possible explanation, that there is a difference in the spatial distribution between bright and faint galaxies, and that the apparent deficit of the surface-density excess is due to the more uniform distribution of the faint cluster galaxies. Indeed, such luminosity segregation is also seen in the spatial distribution of the color-selected galaxies that may be at $z \gtrsim 1.2$, as shown in figure 10 (subsection 3.3). This tendency is insensitive to subtle changes of the boundary between the '$z = 1.2$' and 'foreground' color domains in figure 4. There are several possible origins for such a luminosity segregation. Within the framework of the theory of biased galaxy formation with cold dark matter, luminosity segregation is naturally predicted (Valls-Gabaud et al. 1989). In biased CDM theory, the most massive and oldest galaxies correspond to the highest peaks of the initial density fluctuations, and are concentrated more strongly at the early formation epoch. Alternatively, merger events may play important roles (e.g., Fusco-Femiano, Menci 1998); since galaxy merging may occur more frequently at the dense cluster core, massive galaxies can be formed efficiently in the central region.

The difference in the sky distribution between those galaxies with different colors and magnitudes may be the result of the superposition of two systems, namely those at $z = 1.21$ and 1.15, that may contain different galaxy populations. Postman et al. (1998) indeed show such an example. The cluster Cl 0023+0423 at $z = 0.84$ was revealed to consist of two poor clusters or groups of galaxies; they found that there are few luminous galaxies in one system, while luminous red galaxies exist in the other system. The 3C 324 clusters may be in similar situation to Cl 0023+0423. Although they are not associated with each other in the real space in the case of the 3C324 clusters, there may be a large variety of galaxy populations among the high-redshift clusters or groups.

Finally, we note a rather speculative feature about the galaxy spatial distribution. The large-scale distribution of those galaxies with a '$z = 1.2$' color domain in the field extends in an east–west direction centered at 3C 324, and is aligned with the radio axis of 3C 324. This may imply a possible relationship between the past radio jet activity of 3C 324 and galaxy formation (e.g., West 1994).

We wish to thank Alfonso Aragón-Salamanca, the referee of this paper, for his invaluable comments. The present result is indebted to all the members of the Subaru Observatory, NAOJ, Japan. We thank Nobuo Arimoto for kindly providing the Kodama and Arimoto evolutionary synthesis models. This research was supported by grants-in-aid for scientific research of the Ministry of Education, Science, Sports and Culture (08740181, 09740168). This work was also supported by the Foundation for the Promotion of Astronomy. This work is based in part on observations with the NASA/ESA Hubble Space Telescope, obtained from the data archive at the Space Telescope Science Institute, which is operated by AURA, Inc. under NASA contract NAS5–26555. The Image Reduction and Analysis Facility (IRAF) used in this paper is distributed by National Optical Astronomy Observatories, operated by the Association of Universities for Research in Astronomy, Inc., under contact to the National Science Foundation.

References

Abraham R. G., van Den Bergh S., Glazebrook K., Ellis R. S., Santiago B. X., Surma P., Griffiths R. E. 1996, ApJS 107, 1

Aragón-Salamanca A., Ellis R. S., Couch W. J., Carter D. 1993, MNRAS 262, 764

Benítez N., Broadhurst T., Rosati P., Courbin F., Squires G., Lidman C., Magain P. 1999, ApJ 527, 31

Bertin E., Arnouts S. 1996, A&AS 117, 393

Bower R. G., Kodama T., Terlevich A. 1998, MNRAS 299, 1193

Bower R. G., Lucey J. R., Ellis R. S. 1992, MNRAS 254, 601

Bruzual A. G., Charlot S. 1993, ApJ 405, 538

Butcher H., Oemler A. Jr 1978, ApJ 219, 18

Butcher H., Oemler A. Jr 1984, ApJ 285, 426

Cardelli J. A., Clayton G. C., Mathis J. S. 1989, ApJ 345, 245

Conselice C. J., Bershady M. A., Jangren A. 1999, ApJ in press (*astro-ph*/9907399)

De Propris R., Eisenhardt P. R., Stanford S. A., Dickinson M. 1998, ApJ 503, L45

De Propris R., Stanford S. A., Eisenhardt P. R., Dickinson M., Elston R. 1999, AJ 118, 719

Dickinson, M. 1995, ASP Conf. Ser. 86, 283

Dickinson M. 1997a, in HST and the High Redshift Universe, ed N. R. Tanvir, A. Aragón-Salamanca, J.V. Wall (World Scientific, Singapore) p.207

Dickinson, M. 1997b, in The Early Universe with the VLT, ed J. Bergeron (Springer, Berlin) p274

Dressler A., Gunn J. E. 1992, ApJS 78, 1

Dressler A., Smail I., Poggianti B. M., Butcher H., Couch W. J., Ellis R. S., Oemler A. Jr 1999, ApJS 122, 51

Ellis R. S., Smail I., Dressler A., Couch W. J., Oemler A. Jr, Butcher H., Sharples R. M. 1997, ApJ 483, 582

Fusco-Femiano R., Menci N. 1998, ApJ 498, 95

Garilli B., Bottini D., Maccagni D., Carrasco L., Recillas E. 1996, ApJS 105, 191

Gladders M. D., López-Cruz O., Yee H. K. C., Kodama T. 1998, ApJ 501, 571

Hall P. B., Green R. F. 1998, ApJ 507, 558

HST Data Handbook, Ver3.1 1998, http://www.stsci.edu/documents/data-handbook.html

Kajisawa M., Yamada T. 1999, PASJ 51, 719

Kajisawa M., Yamada T., Tanaka I., Maihara T., Iwamuro F., Terada H., Goto M., Motohara K. et al. 2000, PASJ in press (Paper I)

Kodama T., Arimoto N. 1997, A&A 320, 41

Kodama T., Arimoto N., Barger A. J., Aragón-Salamanca A. 1998, A&A 334, 99

Kristian J., Sandage A., Katem B. 1974, ApJ 191, 43

Motohara K., Maihara T., Iwamuro F., Oya S., Imanishi M., Terada H., Goto M., Iwai J., et al. 1998, Proc. SPIE 3354, 659

Poggianti B. M., Smail I., Dressler A., Couch W. J., Barger A. J., Butcher H., Ellis R. S., Oemler A. Jr 1999, ApJ 518, 576

Postman M., Lubin L. M., Oke, J. B. 1998, AJ 116, 560

Rakos K. D., Schombert J. M. 1995, ApJ 439, 47

Rosati P., Stanford S. A., Eisenhardt P. R., Elston R., Spinrad H., Stern D., Dey A. 1999, AJ 118, 76

Smail I., Dickinson M. 1995, ApJ 455, L99

Smail I., Edge A. C., Ellis R. S., Blandford R. D. 1998, MNRAS 293, 124

Spinrad H., Djorgovski S. 1984, ApJ 280, L9

Stanford S. A., Eisenhardt P. R., Dickinson M. 1998, ApJ 492, 461

Stanford S. A., Elston R., Eisenhardt P. R., Spinrad H., Stern D., Dey A. 1997, AJ 114, 2232

Tanaka I., Yamada T., Aragón-Salamanca A., Kodama T., Miyaji T., Ohta K., Arimoto N. 1999, ApJ in press (*astro-ph*/9907437)

Terlevich A. I., Kuntschner H., Bower R. G., Caldwell N., Sharples R. M. 1999, MNRAS in press (*astro-ph*/9907072)

Valls-Gabaud D., Alimi J.-M., Blanchard A. 1989, Nature 341, 215

van Dokkum P. G., Franx M. 1996, MNRAS 281, 985

van Dokkum P. G., Franx M., Kelson D. D., Illingworth G. D. 1998, ApJ 504, L17

Visvanathan N., Sandage A. 1977, ApJ 216, 214

Wainscoat R. J., Cowie L. L. 1992, AJ 103, 332

West M. J. 1994, MNRAS 268, 79

Yamada T., Tanaka I., Aragón-Salamanca A., Kodama T., Ohta K., Arimoto N. 1997, ApJ 487, L125

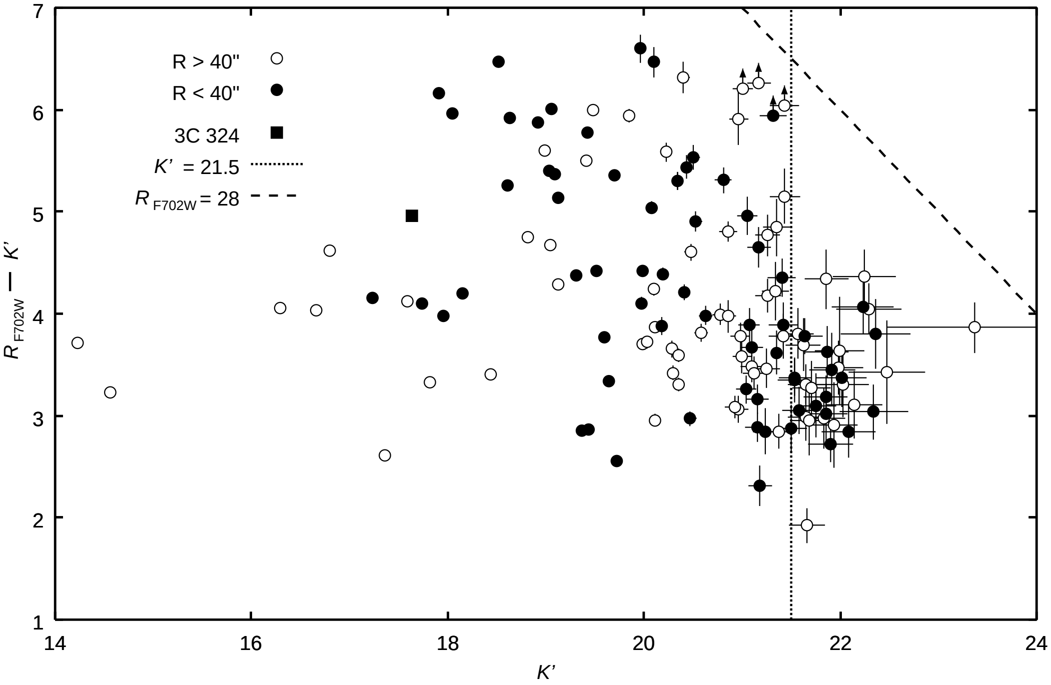

Fig. 1. $R_{\mathrm{F702W}} - K'$ vs K' color–magnitude diagram for the galaxies in the region of 3C 324. The shaded and open circles represent galaxies in the 'cluster' region within 40" of 3C 324, and the adjacent 'outer' region, respectively. 3C 324 is plotted with the solid square. The dotted line represents $K' = 21.5$ mag, and the dashed line shows $R_{\mathrm{F702W}} = 28$ mag (see text).

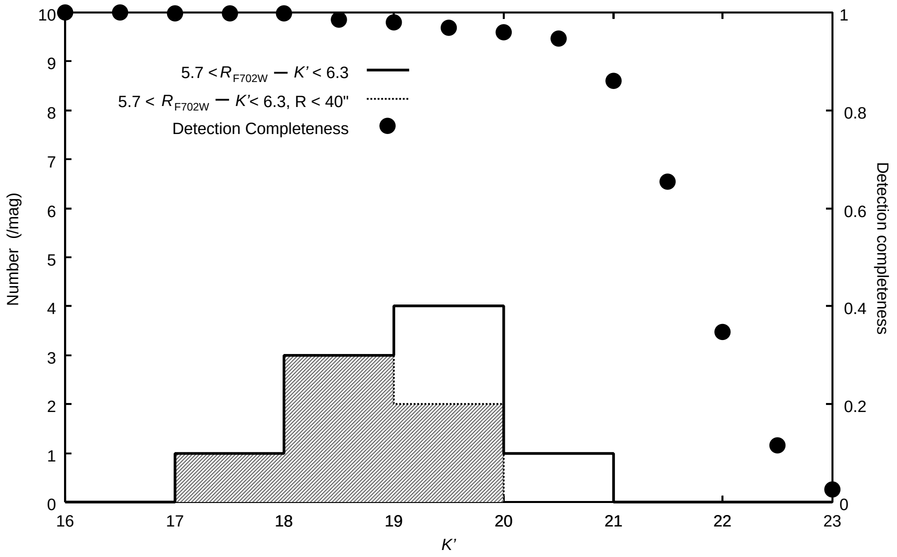

Fig. 2. Number counts of the 'red sequence' galaxies with $5.7 < R_{\mathrm{F702W}} - K' < 6.3$, except for those objects not detected in the R_{F702W}-band image. The hatched region represents those galaxies within 40 arcsec radius of 3C 324. Detection completeness in the K' image is also shown.

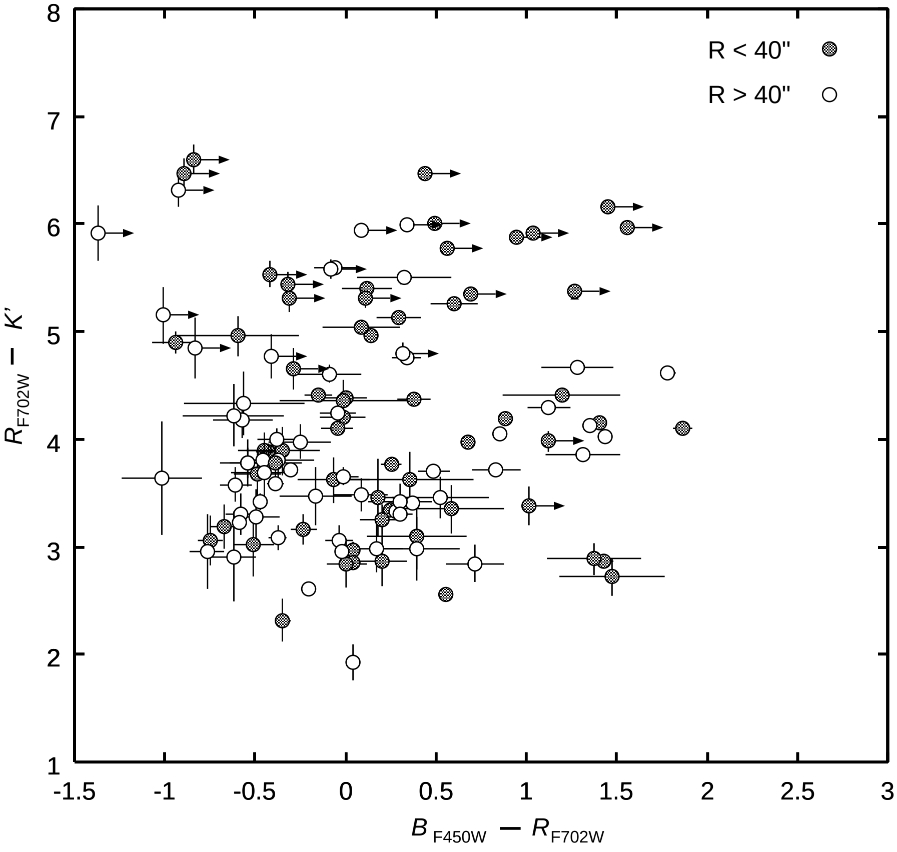

Fig. 3. $R_{\mathrm{F702W}} - K'$ vs $B_{\mathrm{F450W}} - R_{\mathrm{F702W}}$ two-color diagram for the galaxies with $K' < 22$. The meaning of the symbols is similar to those in figure 1.

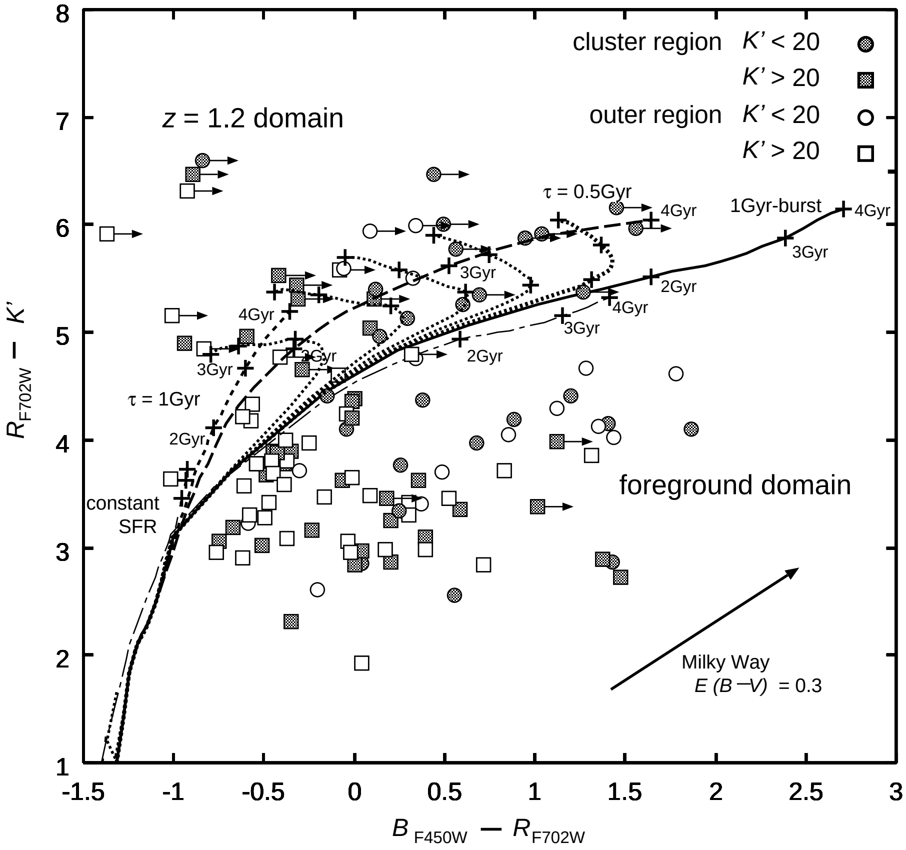

Fig. 4. Same two-color diagram as figure 3, but the galaxies are divided into brighter and fainter samples (circles for $K' < 20$, and squares for $K' > 20$), and the models for the galaxies at $z = 1.2$ with various star-formation histories are plotted along the age sequence. Tracks of the models of 1 Gyr-burst (solid line for solar metallicity and dot-dashed line for 0.2 solar), $\tau = 0.5$ Gyr (long-dashed line), $\tau = 1$ Gyr (short-dashed line), and constant SFR (thin dashed line) are shown. The crosses represent the ages of 2, 3, 4 Gyr. The dotted lines represent the track of old (1 Gyr burst) + ongoing starburst (constant SFR) with mass fractions of 0.02, 0.05, 0.1, 0.2, 0.5% (from right to left). We show the effect of reddening by the large arrow using the galactic extinction curve given in Cardelli et al. (1989) for $E(B - V) = 0.3$.

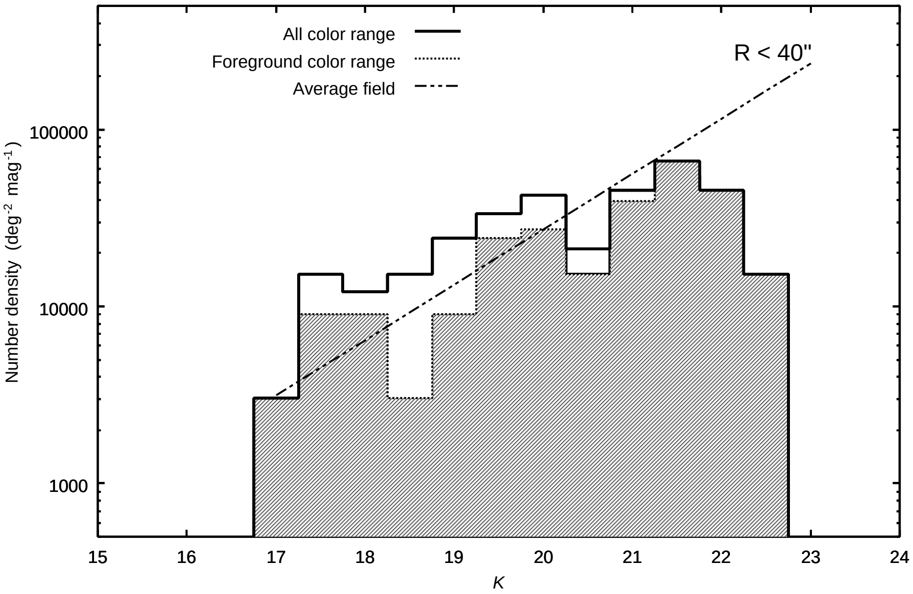

Fig. 5. K-band number counts of galaxies in the 'cluster' region. The hatched region represents those of the galaxies within the 'foreground' color range in figure 4. The dash-dotted line shows the averaged general field counts derived from the literature (Paper I). No color correction is applied in converting the K'-band magnitude to K-band one.

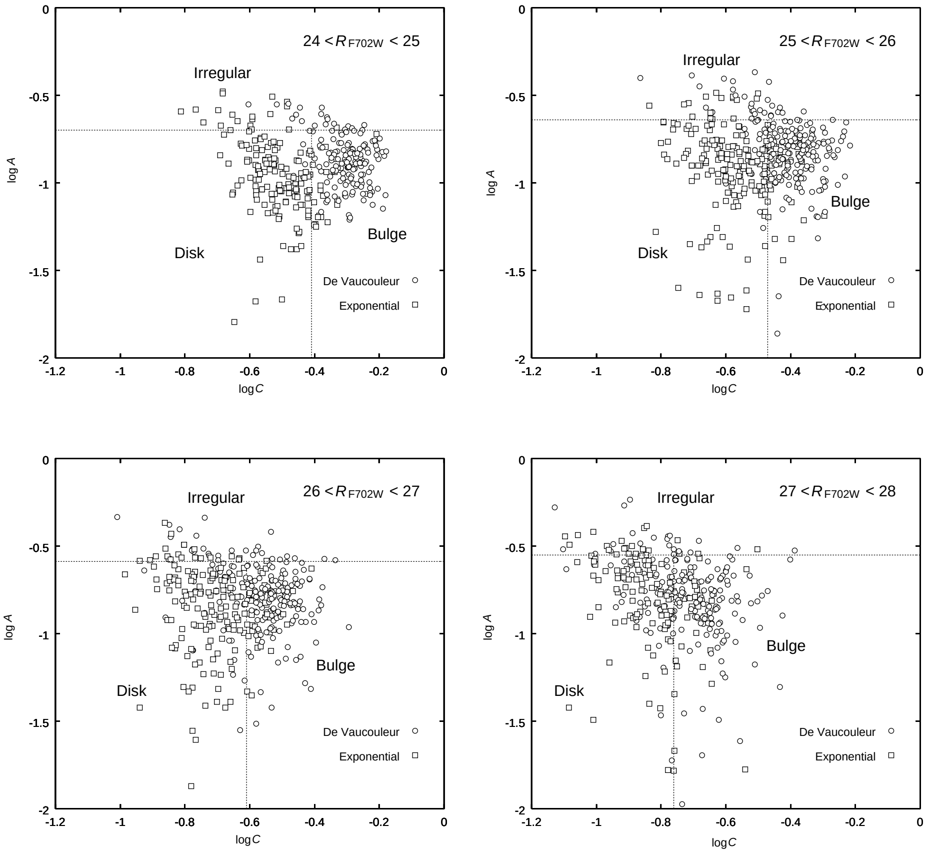

Fig. 6. log C–log A morphological classification for the artificial galaxies on the WFPC2 image shown in each magnitude bin. Each symbol represents the light profile of artificial galaxies. The dotted lines show the boundary between 'bulge', 'disk', and 'irregular' galaxies (see text).

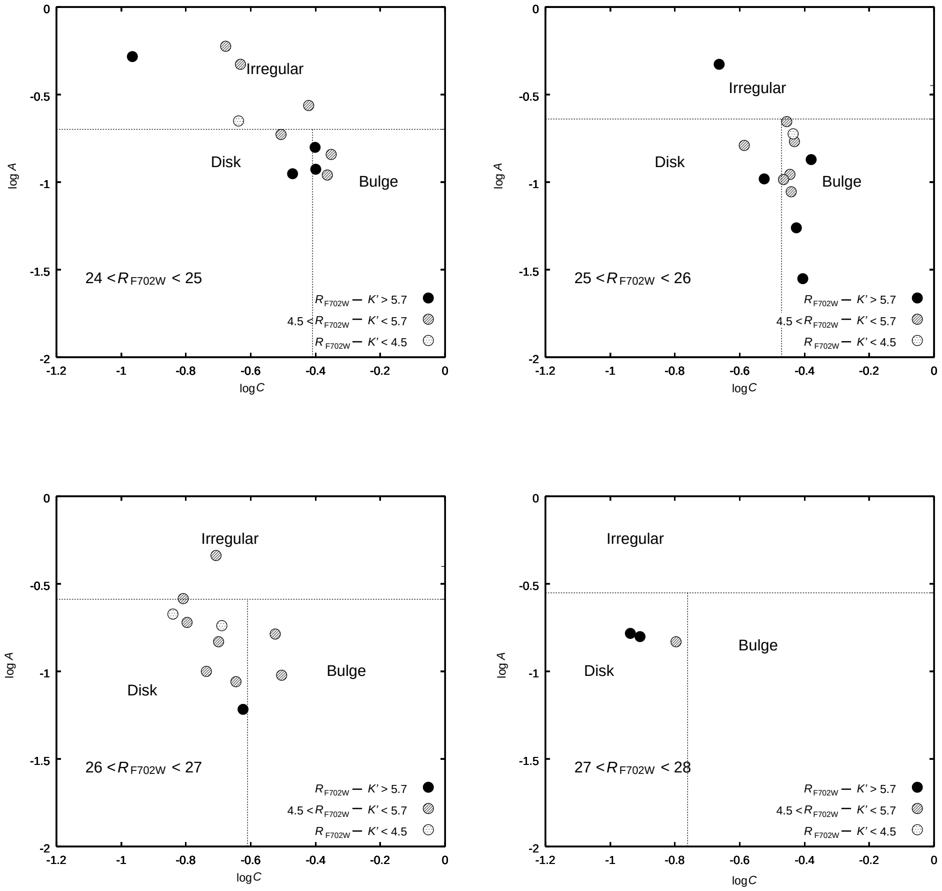

Fig. 7. Morphological classification of the real galaxies within the '$z = 1.2$' color range on the WFPC2 image.

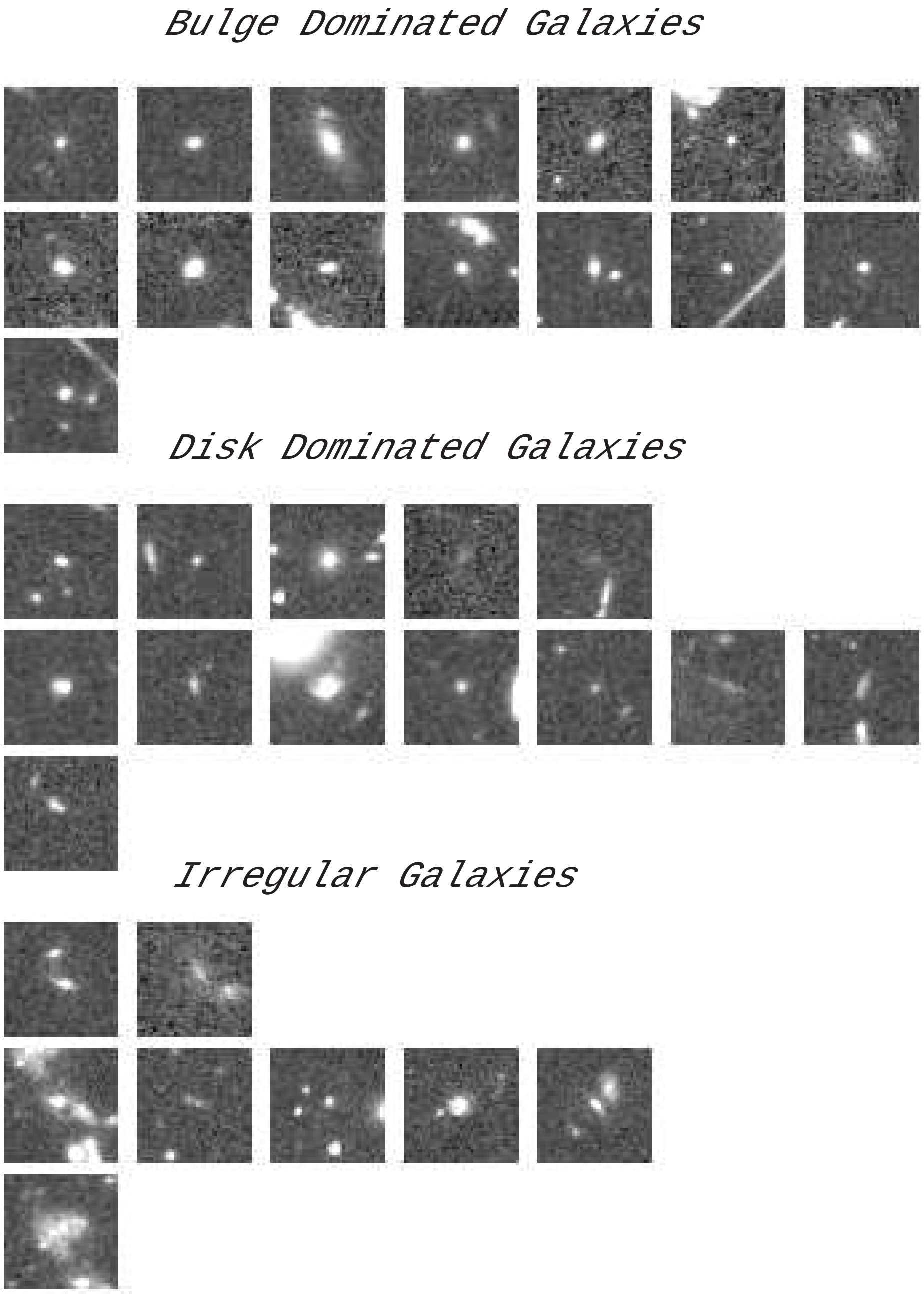

Fig. 8. HST WFPC2 R_{F702W}-band images of the galaxies in figure 7. The top three rows: 'bulge-dominated' galaxies. Middle: 'disk-dominated' galaxies. Bottom: irregular galaxies. In each morphological block, each row represents galaxy color; $R_{\mathrm{F702W}} - K' > 5.5$ (top), $4.5 < R_{\mathrm{F702W}} - K' < 5.5$ (middle), and $R_{\mathrm{F702W}} - K' < 4.5$ (bottom).

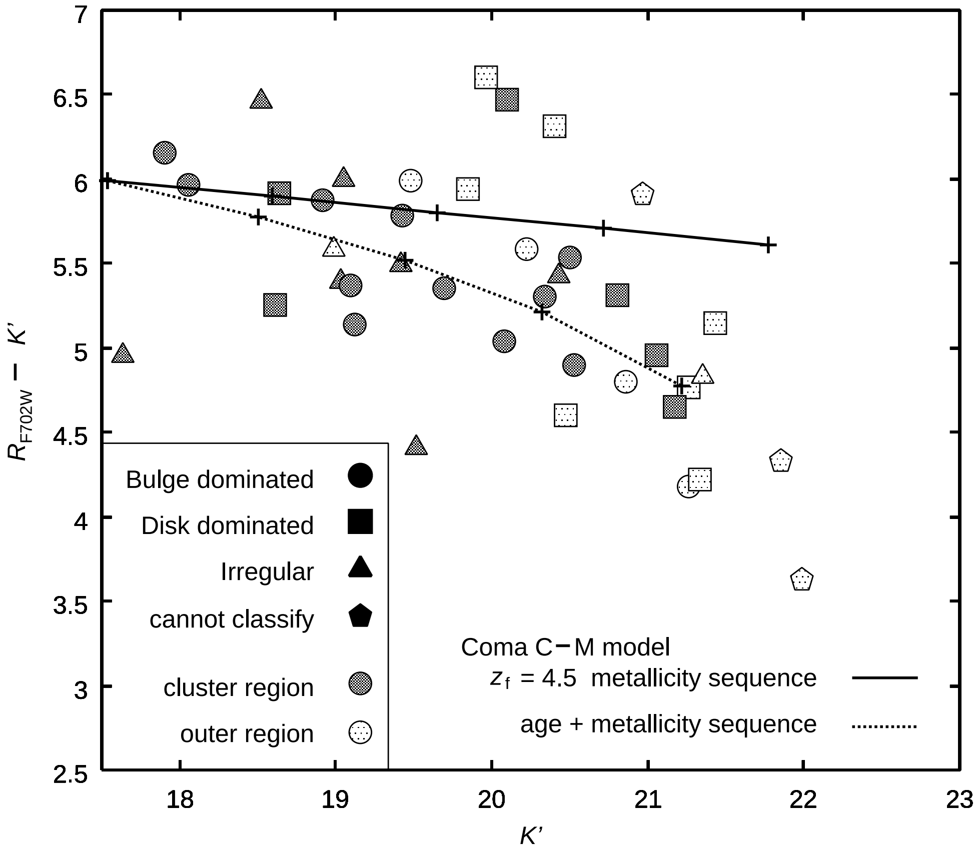

Fig. 9. $R_{\rm F702W} - K'$ vs K' color-magnitude diagram for those galaxies within the '$z = 1.2$' color range in figure 4. The shape of each symbol represents the morphology classified in figure 7. The solid line represents the metallicity-sequence C-M relation model for the Coma cluster (Kodama, Arimoto 1997), which would be observed at $z = 1.2$, assuming passive evolution. The dotted line shows a similar model with a 1–3 Gyr age difference along the sequence (see text).

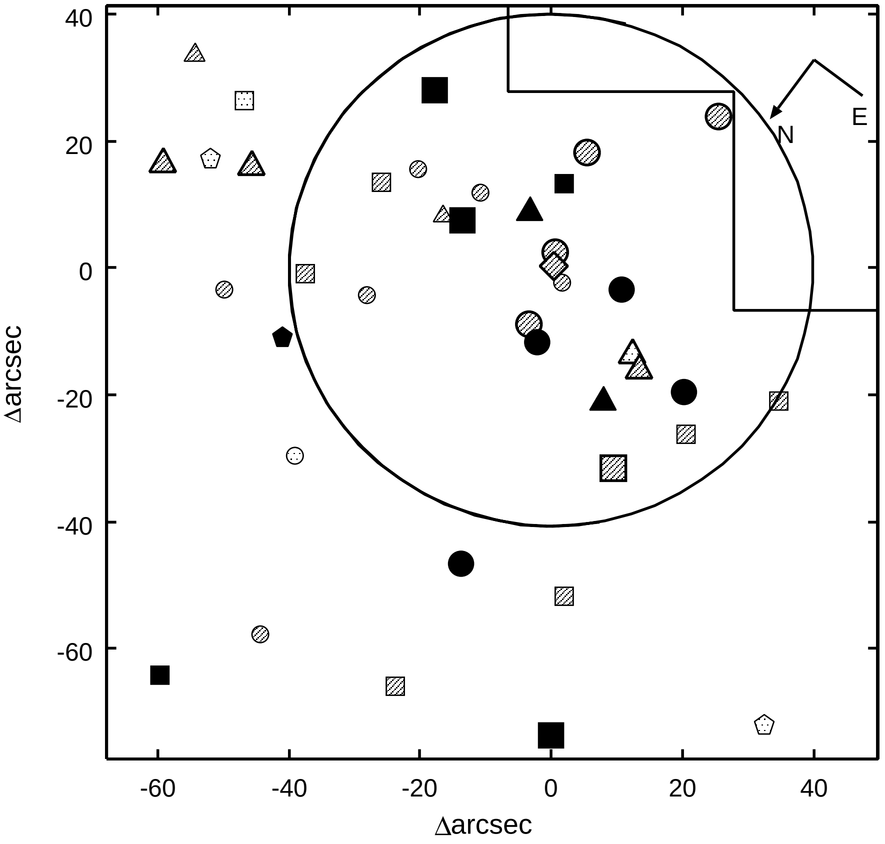

Fig. 10. Spatial distribution of the galaxies within the '$z = 1.2$' color range. The meaning of the shape of each symbol is the same as in figure 9. The size of each symbol represents $K' < 20$ (large), $K' > 20$ (small), respectively. The pattern of each symbol represents $R_{\mathrm{F702W}} - K'$ color, $R_{\mathrm{F702W}} - K' > 5.5$ (filled), $4.5 < R_{\mathrm{F702W}} - K' < 5.5$ (hatched), $R_{\mathrm{F702W}} - K' < 4.5$ (dotted). 3C 324 is plotted with a diamond. The upper light solid line shows the boundary of the optical WFPC2 images. The large solid circle represents a 40-arcsec radius from 3C324.